CFRP-CONFINED REINFORCED CONCRETE ELEMENTS SUBJECTED TO CYCLIC COMPRESSIVE LOADING

By J. A. O. Barros[1], D. R. S. M. Ferreira[2], and R. K. Varma[3]

ABSTRACT

The effectiveness of discrete and continuous CFRP wrapping arrangements for reinforced concrete (RC) short column subjected to monotonic and cyclic compressive loading is assessed in this work. The experimental program is composed of four series of RC columns with discrete wrapping arrangements and one series of full wrapped RC columns. Each series is composed of a monotonic and a cyclic test. Strain gauges were installed along the height of each column to measure the strain field in the CFRP during the test. The variation of the stiffness of the unloading and reloading branches of each loading cycle was determined. A constitutive model to simulate FRP-confined RC concrete elements subjected to cyclic compressive loading was developed and implemented into a computer program based on the finite element method. This model was appraised with the data obtained from the carried out experimental program.

KEYWORDS: Carbon Fiber Reinforced Polymers, Concrete Confinement, Columns, Wrapping, Cyclic Loading, cyclic constitutive model, FEM.

[1] **Joaquim Barros** is Associate Professor and Director of the Laboratory of the Structural Division of the Department of Civil Engineering, University of Minho, Portugal. He is a Member of ACI Committees 440 and 544, a Member of *fib* TG 9.3 and TG 8.3, and a Council Member of the IIFC. His research interests include structural strengthening, composite materials, fiber reinforced concrete and finite element method.

[2] **Debora Ferreira** is a PhD Student in the Structural Division of the Department of Civil Engineering, University of Minho. Her main interests are structural strengthening with composite materials.

[3] **Rajendra Varma** is a PhD Student in the Structural Division of the Department of Civil Engineering, University of Minho. His main interests are the development of constitutive models to simulate the material nonlinear behavior or reinforced concrete structures strengthened by FRP composite materials, using finite element method and computational mechanics.

INTRODUCTION

Wrapping reinforced concrete (RC) columns with wet lay-up carbon fiber reinforced polymer (CFRP) sheets, using discrete (strips in between the existent steel hoops) or continuous (full wrapping) confinement arrangements, has proven to be an effective strategy to increase the load carrying capacity, ultimate deformability and energy absorption capacity of RC columns. The increase in terms of the energy that an RC column can dissipate before its collapse, due to the concrete confinement provided by CFRP arrangements, is one of the main reasons justifying the appropriateness of these composite materials to retrofit RC columns of the built heritage located in zones of high seismic risk [1-4].

To preserve the global structural stability of buildings located in these zones, it is mandatory to assure that their columns do not fail when subjected to a seismic event. When this type of event occurs, the columns are subjected to cyclic compressive loading. To explore the potentialities of CFRP-confinement arrangements to increase the load carrying capacity and energy absorption ability of RC columns subjected to cyclic compressive loading, an experimental program was carried out with RC column specimens having a cross section of 200 mm diameter and a height of 600 mm. The influence of the CFRP confinement arrangement on the cyclic compressive behavior of concrete was evaluated.

Predicting the behavior of CFRP-confined RC columns submitted to seismic loading is a complex task, requiring sophisticated constitutive models able of reproducing the behavior of the intervening materials up to their collapse, and FEM-based computer programs that include the algorithms associated to the material nonlinear analysis of RC structures. However, the development of these numerical tools is mandatory since their use can avoid the execution of too expensive experimental programs and can help the designer on the selection of the best strengthening strategies to adopt. To give a contribution in this domain, a CFRP-confined concrete cyclic constitutive model was developed and implemented into a FEM-based computer program. The results from the experimental program were used to calibrate some variables of this model and to appraise its performance.

CONFINEMENT ARRANGEMENTS AND EXPERIMENTAL PROGRAM

The present work is part of a research program that aims at developing guidelines for the design of discrete and continuous FRP confinement arrangements to RC columns submitted to monotonic and cyclic loadings. In previous works [5,6], the most effective discrete confinement arrangements were selected, taking into account the increment in terms of load carrying and energy absorption capacities provided by discrete and continuous confinement configurations, as well as the labor time and materials these arrangements require. The present work deals with the most effective discrete confinement arrangements and compares their performance with that obtained from continuous confinement arrangements. These arrangements are schematically represented in Table 1. Each specimen is designated as WiLk_c/m, where Wi represents the strip width and Lk the number of CFRP layers per each strip. To distinguish cyclic from monotonic tests, a c letter was attributed to a specimen submitted to cyclic tests, while an m letter was used to designate monotonic tests. Each series of direct compression tests (WiLk*)* was composed of two specimens, one submitted to monotonic loading (WiLk_m) while the other was submitted to cyclic loading (WiLk_c). Figure 1 shows the confinement arrangements adopted in this work. A detailed description of the confinement procedures can be found elsewhere [7].

MATERIALS

CFRP sheets with the trade name of Mbrace CF-120 (200 g/m^2 of fibers) were used in the present experimental program. These sheets had 0.113 mm of thickness, a tensile strength of 3539 MPa, an elasticity modulus and an ultimate strain in the fiber's direction of 232 GPa and 1.53%, respectively. To evaluate these properties, samples of the CFRP sheet were tested in compliance with the ISO recommendations [8].

To determine the values of the properties that characterize the tensile behavior of used steel bars, five tensile tests for each steel bar diameter were carried out according to the NP-EN 10 002-1 recommendations [9]. The average values of the obtained results are the following: for the steel hoops of 6 mm diameter, a yield stress (σ_{sy}) of 468.3 MPa, a tensile strength (σ_{su}) of 616.2 MPa, an elasticity modulus (E_s) of 212.2 GPa and an ultimate strain (ε_{su}) of 8%; for the longitudinal steel bars of 8 mm diameter, σ_{sy}=517.2 MPa, σ_{su}=607.9 MPa, E_s=199.8 GPa and ε_{su}=11%.

The concrete compressive strength was determined according to NP-EN 12 390-3 [10]. From tests on 150 mm cubes, an average compressive strength of 30 MPa was obtained at 28 days.

TEST SETUP

The cyclic and monotonic direct compression tests were carried out using a closed-loop test machine of 2250 kN maximum load capacity. Specimen axial deformation was measured by means of LVDTs clamped to the steel load platens of the equipment, as shown in Figure 2. Strains in the CFRP fiber direction were measured by strain gauges (SG) placed according to the schemes presented in Table 1.

The specimens subjected to cyclic compressive load were tested under force control at a load rate of 15 kN/s, according to the loading history schematically

represented in Figure 3. The last test procedure consisted of a ramp in displacement control up to the rupture of the specimen.

The specimens subjected to monotonic loading were tested under displacement control at a displacement rate of 5 μm/s, using an external LVDT of 20 mm of measuring length. The test was stopped when the measuring length of the LVDT was reached.

EXPERIMENTAL RESULTS

The main effectiveness indicators for the adopted confinement systems are included in Table 2, where f_{cc} is the maximum concrete compressive stress, f_{cc}^{URC} and f_{cc}^{CRC} are the compressive strength of unconfined and confined reinforced specimens, ε_{cc} is the specimen axial strain at f_{cc}, ε_{cc}^{CRC} and ε_{cc}^{URC} are the specimen axial strain at f_{cc}^{CRC} and f_{cc}^{URC}, respectively, and ε_{fmax} is the maximum tensile strain in the CFRP fiber's direction. The variation of W and L leads to specimens with different values for the CFRP volumetric ratio, ρ_f, which is evaluated from:

$$\rho_f = 4\frac{W\ L\ S\ t_f}{D\ H} \tag{1}$$

where t_f is the thickness of the CFRP sheet and D and H represent, respectively, the diameter and the height of the specimen. In Table 2, UPC represents the unconfined plain concrete specimens and URC the specimens reinforced with longitudinal and transversal steel bars, without any CFRP confinement arrangement.

From the analysis of the results included in Table 2 the following observations can be outlined:

- The specimen load carrying capacity rises with the increase of ρ_f. Taking as basis of comparison the f_{cc} values of URC specimen (f_{cc}^{URC}) it is observed that $f_{cc}^{CRC}/f_{cc}^{URC}$ ratio varied between 1.5 for ρ_f=0.31 and 2.68 for ρ_f=0.68. Regardless of the loading type, a tendency of $f_{cc}^{CRC}/f_{cc}^{URC}$ ratio to increase with the increase of ρ_f is noted;

- Comparing the results of specimens of equal ρ_f subjected to cyclic loading, it can be concluded that full-wrapping is more effective than discrete confinement arrangements. Similar tendency was expected for the specimens subjected to monotonic loading, as previous research has already proved 5, but W600L3_m specimen presented a too abnormal low load carrying capacity, which might have been caused by a deficient application of the CFRP system or an incorrect position of this specimen in the testing machine, resulting some eccentricity of the applied load. The lower effectiveness of discrete confinement systems can be justified by the accumulated damage in the unconfined concrete between strips. This effect is more pronounced in specimens subjected to cyclic loading, since the concrete plastic strain increases in subsequent cycles of the series of cycles of same load amplitude (see Figure 4). However, it should be noted that, in

comparison with the full wrapping confinement system, the partial confinement arrangements are easier and faster to apply 7;

- If the W600L3_m specimen is excluded from the analysis, the $\varepsilon_{cc}^{CRC}/\varepsilon_{cc}^{URC}$ ratio has a tendency to rise with the increase of ρ_f (a negative signal attributed to the concrete compressive strain). Due to the accumulation of the concrete compressive plastic strain, mainly in between CFRP strips in subsequent loading cycles, values of the $\varepsilon_{cc}^{CRC}/\varepsilon_{cc}^{URC}$ ratio were larger in the specimens submitted to cyclic loading than in the specimens under monotonic loading;

- There was a tendency for maximum CFRP strains (a positive signal attributed to the CFRP tensile strains) to occur in the top half of the specimen, in spite of a large dispersion within the obtained results, since these measures are restricted to the influence area of the SGs and they can be even affected by localized occurrences. A similar tendency has, however, already been reported by other authors 11,12. In fact, failure occurs, in general, by the rupture of the CFRP strips located in the upper half of the specimen, mainly in the first and/or second strips.

Figure 4 shows the curves that relate the concrete axial compressive stress (f_c) with the concrete axial compressive strain (ε_c) in the specimens submitted to cyclic (WiLk_c) and monotonic (WiLk_m) loadings. In Figure 4, the relationship between f_c and the average strain in the CFRP strips (ε_{fm}) is also included for both monotonic and cyclic tests (the strains were not measured in the W60L3_c test due to the malfunctioning of the SG data acquisition system).

Figure 4 shows that:

- the curve of the monotonic test can be regarded as the envelope of the curve of the corresponding cyclic test;

- In each series of load cycles, both the concrete axial strain and the average CFRP strain increased from the first to the third cycle. The increase of the concrete axial strain can be justified by concrete dilation, mainly at the zones in-between CFRP strips, while the increase of the CFRP tensile strain can be justified by the increase of concrete plastic strain in subsequent load cycles. In fact, the recovered strain in the unloading branch of each cycle is only a part of the strain increment occurred in the reloading branch of the previous cycle, which means that an increment of strain is installed in the CFRP in subsequent load cycles;

- In general, the maximum load attained in the reloading branch of the 1st load cycle of each series of load cycles was higher than the load carrying capacity (for equal level of axial deformation) of the homologous specimens submitted to monotonic loading. Due to the increase of tensile strains in the CFRP in subsequent load cycles of each series of load cycles, an increase of confinement pressure is introduced into concrete by the CFRP system, leading that the reloading branch of the last cycle of each series of load cycles (the returning to the monotonic phase) presents higher load carrying capacity. As expected, this occurrence was more pronounced in the full-wrapped specimens;

- From the analysis of the configuration of the f_c-ε_c unloading and reloading branches of each load cycle, it is verified that the unloading branch is eminently non linear, while the reloading branch is formed by nonlinear segments of reduced amplitude at its extremities, connected by a linear part. To evaluate the variation of the stiffness of the unloading and reloading phases of the load cycles along the test, it was assumed that both the unloading and reloading phases could be modeled by linear branches, as shown in Figure 5 (r for the reloading branch and u for the unloading branch).

Figure 6 shows the relationship between the concrete axial strain and the stiffness of the unloading and the reloading branches of the load cycles (secant stiffness). The following observations can be pointed out:

- In each series of load cycles, in the consecutive cycles the stiffness of the unloading and reloading branches shows a tendency to decrease and to increase, respectively. The stiffness increment of the reloading branches is due to the increase of the confinement pressure applied by the CFRP to the concrete in the consecutive cycles. However, this tendency of increase is not as pronounced as the tendency of decrease reported for the unloading branches;

- In the successive series of load cycles, a tendency for a decrease of the stiffness of both the unloading and reloading branches is observed in all tested specimens. The decreased level of the stiffness of these branches diminished with the increase of the specimen axial deformation. This is more pronounced in the full-wrapped specimens, which presented a variation that can be simulated by an exponential law (see Figure 6e). The stiffness of the unloading and reloading branches seems to approach a constant value (residual stiffness). In case of fully wrapped specimens, this value is almost the same for both the unloading and reloading branches, while in the specimens with discrete confinement arrangements the residual stiffness of the unloading branches is higher than that of the reloading branches. This can be justified by the dilation of the unconfined concrete in-between CFRP strips.

Figure 7 shows the curves corresponding to the relationship of the concrete axial compressive stress with both the concrete axial compressive strain and the CFRP tensile strain in the fiber's direction, for the partially confined W60L5 and fully confined W600L3 series, both series with equal ρ_f (see Table 2). To make the figure legible, only the strains recorded by SG2 were included in this graph, once the specimen rupture occurred in the zone where SG2 was installed (see Table 1 and Figure 8). Although partial wrapping arrangements were not as effective in terms of load carrying capacity as full wrapping arrangements, they provided a significant increase of the specimen load carrying capacity (up to two times the compressive strength of its corresponding unconfined specimen). Furthermore, partial wrapping arrangements assured a high level of deformability at the specimen failure, ensured easier and faster application and prevented the rupture modes from being as violent as those of the fully wrapped specimens, since part of the internal energy was gradually dissipated due to the compression strain-softening behavior of the concrete in-between CFRP strips. The shape of the unloading and reloading branches seems to be similar in both partially and fully confined specimens.

After rupture, the partially and fully wrapped specimens of equal ρ_f presented the appearance shown in Figure 8. Failure mode occurred with a violent CFRP rupture, which tended to be more violent as the volume of unconfined concrete between the CFRP strips decreased. This can be justified due the accumulation of plastic deformation of the concrete in these areas.

Figure 9 shows the tensile strains measured in the strain gauges (SG) installed on W60L5 and W600L3 specimens (of equal ρ_f), submitted to cyclic and monotonic loadings, for a load level near the failure of these specimens. In spite of the difficulty in finding a tendency, in general, the maximum strains in the CFRP occurred at the top of the specimens. Since a steel hinge was used at the top of the specimens to transfer the load applied by the machine, the reduced restrain provided by this hinge has allowed SG1 to record the highest gradient of strains (see Figure 9), which justifies the prevalence of the failure of the specimen due to the rupture of the CFRP strip near the location of this SG. Nonetheless, the strains varied from 0.3% up to 1.2%, and the average strain, taking into account the measures registered in all SG of the tested specimens, was approximately 0.7%. This value may be even higher since the strain values registered in the CFRP only represent the areas where the strain gauges are placed, and, consequently, they are too dependent on the specimen failure mode configuration.

Figure 10 represents the relationship between the concrete axial compressive stress and the average strain in the SGs of W60L5 and W600L3 specimens for both the monotonic and cyclic tests. The envelope curve of the cyclic test follows approximately the curve of the monotonic test of the corresponding specimen. However, in general, the envelope stress-strain curve of the cyclic test reveals a higher load carrying capacity than the one of the corresponding monotonic test. This is justified by the pre-stress applied in the CFRP in the consecutive load cycles, which increased the specimen axial stiffness, resulting in higher load carrying capacity of the specimen.

CONSTITUTIVE MODEL FOR FRP-CONFINED CONCRETE SUBJECTED TO CYCLIC COMPRESSION LOADING

The developed model is composed by an envelope and cyclic branches.

Compressive envelope curve

The envelope curve for compression is derived from Lam and Teng model[13]. The stress-strain relationship of the envelope curve (Figure 11) for compression, $f_c - \varepsilon_c$, can be described as follows (compression stresses and strains are assumed with positive sign):

$$f_c = E_c\varepsilon_c - \frac{(E_c - E_{c2})^2}{4f_{co}}\varepsilon_c^2 \text{ and } E_{ct} = E_c - \frac{(E_c - E_{c2})^2}{2f_{co}}\varepsilon_c \quad \text{if} \quad 0 \le \varepsilon_c \le \varepsilon_{ct}; \tag{2}$$

$$f_c = f_{co} + E_{c2}\varepsilon_c \text{ and } E_{ct} = E_{c2} \text{ for } \varepsilon_{ct} \le \varepsilon_c \le \varepsilon_{cc}^{CPC}; \tag{3}$$

where f_{co} is the compressive strength of unconfined plain concrete (UPC), E_c is the concrete initial Young's modulus, ε_{ct} is the strain at the transition between the

domain of the equation (2) and (3), ε_{cc}^{CPC} is the ultimate strain of confined plain concrete (CPC) and:

$$\varepsilon_{ct} = \frac{2 f_{co}}{\left(E_c - E_{c2}\right)} \tag{4}$$

E_{c2} is the tangential Young's modulus determined by:

$$E_{c2} = \frac{f_{cc}^{CPC} - f_{co}}{\varepsilon_{cc}^{CPC}} \tag{5}$$

From experimental results it was verified that the compressive strength of confined plain concrete (f_{cc}^{CPC}) and its corresponding strain (ε_{cc}^{CPC}) can be obtained from:

$$f_{cc}^{CPC} = (1.8244\rho_f + 0.9431) f_{co} \tag{6}$$

$$\varepsilon_{cc}^{CPC} = (-14.696\rho_f^2 + 23.691\rho_f - 2.0105)\varepsilon_{co} \tag{7}$$

Cyclic hysteretic schemes

The hysteretic branches of the proposed cyclic model include nonlinear unloading/reloading, arbitrary cyclic loading and stiffness degradation resulting from cyclic loading. The shape of all possible cyclic branches (complete or partial) is predicted by the transition curve proposed by Chang and Mander [14]:

$$f_c = f_{ca} + (\varepsilon_c - \varepsilon_{ca})[E_{ca} + A_c \left|\varepsilon_c - \varepsilon_{ca}\right|^{R_c}] \tag{8}$$

where R_c is the parameter governing the curvature of the hysteretic branch and A_c is a internal parameter:

$$R_c = \frac{E_{cb} - E_{c\sec}}{E_{c\sec} - E_{ca}},\ A_c = \frac{E_{c\sec} - E_{ca}}{\left|\varepsilon_{cb} - \varepsilon_{ca}\right|^{R_c}} \text{ and } E_{\text{csec}} = \frac{f_{cb} - f_{ca}}{\varepsilon_{cb} - \varepsilon_{ca}} \tag{9}$$

where E_{csec} represents the secant modulus, E_{ca} and E_{cb} are the tangent Young's Modulus at the initial (A) and target (B) points (see Figure 11), and f_{ca} and f_{cb} are the compression stresses at A and B points, respectively.

The proposed compressive cyclic mode, shown in Figure 11 with all the possible hysteretic schemes, can be broadly categorized as: complete unloading (**AB**); partial unloading (**AB'**); complete reloading (**BCD**) and; partial reloading (**B'C'D'**).

Unloading from point **A** (ε_{cun}, f_{cun}) with reversal slope E_{cun} (= $2E_c$, see Figure 11), will target point **B** (ε_{cpl}, 0) with target slope E_{cpl}, whose characteristic parameters can be determined as follows:

$$E_{c\sec} = E_c \left(\frac{\left| \frac{f_{cun}}{E_c \varepsilon_{co}} \right| + 0.57}{\left| \frac{\varepsilon_{cun}}{\varepsilon_{co}} \right| + 0.57} \right),\ E_{cpl} = 0.1 E_c \exp\left(-2 \left| \frac{\varepsilon_{cun}}{\varepsilon_{co}} \right| \right) \text{ and } \varepsilon_{cpl} = \varepsilon_{cun} - \frac{f_{cun}}{E_{c\sec}} \tag{10}$$

The transition curve Eq. (8) is used to join the initial point **A** and the target point **B**. A reversal from any point in between **A** and **B** will initiate the starting of a reloading branch. The complete reloading curve is described by three points (initial point **B**, intermediate point **C** and target point **D**), and two connecting transition curves. The first transition curve connects point **B** (ε_{cpl}, 0) with starting slope E_c, to an intermediate point **C** (ε_{cun}, f_{cnew}) with slope E_{cnew}. Similarly, the second transition curve connects intermediate point **C** to the return point **D** (ε_{cre}, f_{cre}) with target slope E_{cre}. The parameters required for complete reloading are derived from the following Eqs. (see Figure 11):

$$f_{cnew} = f_{cun} - \Delta f_c \tag{11}$$

$$E_{cnew} = \frac{f_{cnew}}{\varepsilon_{cun} - \varepsilon_{cpl}} \tag{12}$$

$$\varepsilon_{cre} = \varepsilon_{cun} + \Delta\varepsilon_c \tag{13}$$

$$E_{cre} = E_c\left(\varepsilon_{cre}\right) \text{ and } f_{cre} = f_c\left(\varepsilon_{cre}\right) \tag{14}$$

$$\Delta f_c = 0.09 f_{cun}\sqrt{\left|\frac{\varepsilon_{cun}}{\varepsilon_{co}}\right|} \text{ and } \Delta\varepsilon_c = 0.1992\ \varepsilon_{cun} \tag{15}$$

For reloading followed by partial unloading, a modified returning point is defined, which is calculated from the modified form of Eqs. (11-15), as described elsewhere [14].

Numerical Simulation

A fibrous model with cyclic constitutive laws for CFRP-confined concrete and steel bars was implemented into FEMIX computer program, which is based on the finite element method (FEM). This model is capable of analysing the nonlinear cyclic behaviour of three-dimensional RC frames, since the beams and columns are simulated by 3D Timoshenko finite elements. Each element is discretized in fibres along its longitudinal direction.

Model appraisal

To verify the capabilities of the proposed model on the simulation of CFRP-confined RC columns submitted to cyclic compressive loading, the carried out tests are simulated, and the experimental and numerical axial stress-strain curves are compared. The values of the model parameters used on the numerical simulations are the following ones: E_c= 30 GPa, f_{co} = 30.2MPa and ε_{co} = 0.004 (mm/mm). All the simulated columns were discretized in three isoparametric Timoshenko finite elements of three nodes each. An integration scheme of two Gauss integration points per finite element was adopted for the evaluation of both the stiffness matrix and internal forces. Every cross section was discretized in forty-eight quadrilateral elements of eight nodes for the confined concrete, and four quadrilateral elements of four nodes to simulate the steel bars, using an integration scheme based on 2×2 Gauss integration points.

Figures 12a-c show that the proposed model simulates with satisfactory accuracy the experimental curves. In spite of predicting the envelope curve with high accuracy the analysis tends to predict a slightly less stiffness and underestimates the energy dissipation capacity of the structure due to the assumption of perfect bond between concrete and steel bars.

CONCLUSIONS

The present work compares the efficacy provided by continuous and discrete confinement arrangements for reinforced concrete (RC) column elements subjected to monotonic and cyclic compressive loading.

Taking the compressive strength obtained in the unconfined reinforcement concrete (URC) specimens (f_{cc}^{URC}) for basis of comparison, a significant increase in the specimen load carrying capacity was provided by the adopted confinement systems provided, since $f_{cc}^{CRC} / f_{cc}^{URC}$ varied between 1.5 for ρ_f=0.31 up to 2.7 for ρ_f=0.68, where f_{cc}^{CRC} is the compressive strength of the corresponding confined specimen.

The $\varepsilon_{cc}^{CRC} / \varepsilon_{cc}^{URC}$ ratio increased with ρ_f, having varied from 7 up to 10, where ε_{cc}^{URC} and ε_{cc}^{CRC} are the strains of unconfined reinforced concrete specimen and confined specimen, respectively.

Comparing the results obtained in specimens of equal ρf it was verified that the load carrying capacity of partially confined specimens (W60L5) was a little bit lower than that of the fully confined specimens (W600L3). However, it should be kept in mind that partial confinement arrangements were easier and faster to apply than full confinement arrangements. The obtained stress-strain curves indicate that the curve corresponding to the monotonic test can be considered as the envelope of the curve of the cyclic test.

Regarding the variation of the stiffness of the unloading and reloading branches of the load cycles, it was noticed that the stiffness of the unloading branches was higher than the stiffness of the reloading branches. In the consecutive cycles of a series of cycles with the same load amplitude, the stiffness of unloading branches decreased, while the stiffness of the reloading branches presented a tendency to increase. Finally, a tendency was observed for a decrease in the stiffness of both the unloading and reloading branches in successive series of load cycles.

The data obtained from the experimental program was used to appraise a model proposed to simulate the cyclic behavior of CFRP-confined RC columns. The model simulated with high accuracy the carried out tests.

ACKNOWLEDGEMENTS

The authors of the present work wish to acknowledge the materials supplied by S&P Clever Reinforcement and MBT Bettor Portugal. The second author would like to thank the financial support by PRODEP action 5.3/N/199.014/01. The third author acknowledges the grant obtained in the ambit of the research project "CUTINSHEAR - Performance assessment of an innovative structural FRP strengthening technique using an integrated system based on optical fibre sensors", Reference: POCI/ECM/57518/2004.

REFERENCES

1. Seible, F.; Priestley, M. J. N.; Hegemier, G. A., and Innamorato, D., "Seismic retrofit of RC columns with continuous carbon fiber jackets", ASCE, Journal of Composites for Construction, Vol. 1, nº2, pp. 52-62, 1997.

2. Mirmiran A., and Shahawy M., “Behaviour of concrete columns confined by fiber composites”, ASCE Journal of structural Engineering, Vol 123, nº5, pp. 583-590, 1997.

3. Saadatmaneh, H.; Ehsani, M.R, and Jin, L., “Repair of earthquake-damage RC columns with FRP wraps”, ACI Structural Journal, Vol. 94, No. 2, , pp. 206-214, March-April 1997.

4. Pantelides, P. C.; Gergely, J., “Carbon fiber reinforced polymer seismic retrofit of RC bridge bent: design and in situ validation”, ASCE Journal of composites for construction, Vol. 6, No. 1, pp. 52-60, February 2002.

5. Barros, J.A.O., and Ferreira, D.R.S.M., “Assessing the efficiency of CFRP discrete confinement systems for concrete column elements”, in appreciation for eventual publication in the Journal of Composites for Construction, 2007.

6. Ferreira, D.R.S.M., and Barros, J.A.O., “Confinement efficacy of partially and fully wrapped CFRP systems in RC column prototypes”, 2nd International fib Congress, Naples, June 5-8, Article 10-20 in CD, 2006.

7. Ferreira, D.R.S.M., and Barros, J.A.O., “Discrete and full confinement of concrete elements with CFRP sheets”, Technical Report, 04-DEC/E-29 Dep. Civil Eng. University of Minho, 165 p, 2004. http://www.civil.uminho.pt/composites. (in Portuguese).

8. ISO TC 71/SC 6 N, “Non-conventional reinforcement of concrete-test methods-Part 2: Fiber reinforced polymer (FRP) sheets”, International Organization for Standardization (ISO), Geneva, Switzerland, 2003.

9. NP-EN 10 002-1, “Metallic materials - Tensile testing. Part 1: Method of test (at ambient temperature)”, European Standard, CEN, Brussels, Belgium, pp. 35, 1990.

10. NP-EN 12 390-3, “Testing hardened concrete - Part 3: Compressive strength of test specimens”, European Standard, CEN, Brussels, Belgium, pp. 1, 2002.

11. Rodrigues C.C., and Silva, G.M., “Behaviour of GFRP reinforced concrete columns under monotonic and cyclic axial compression”, Int. Conf. Composites in Construction, Balkema, Porto, pp.245-250, October 2001.

12. Triantafillou, T.C, “Seismic retrofitting of structures with fibre-reinforced polymers”, Prog. Struct. Engng Mater., vol.3, 57-65, 2001.

13. Lam, L., and Teng, J.G., “Design-oriented stress-strain model for FRP-confined concrete”, J. Construction and Building Materials, Elsevier, vol. 17, 471-489, 2003.

14. Chang, G.A., Mander, J.B., “Seismic energy based fatigue damage analysis of bridge columns: Part I-Evaluation of seismic capacity”, Tech. Report NCEER-94-0006, 1994.

NOTATION

$CFRP$	=	carbon fiber reinforced polymers
CPC	=	confined plain concrete
CRC	=	confined reinforced concrete
D	=	diameter of the column cross section
E_s	=	elasticity modulus of the steel bars
E_c	=	initial Young modulus of concrete
E_{cnew}	=	tangent modulus at the new stress point
E_{cpl}	=	tangent modulus when the stress is released
E_{cre}	=	tangent modulus at the returning point (ε_{cre},f_{cre})
E_{ct}	=	tangent modulus for concrete on compression envelope
f_c	=	concrete compressive stress
f_{cc}	=	compressive strength of confined concrete
f_{co}	=	compressive strength of UPC
f_{cnew}	=	new value of stress corresponding to the unloading strain(ε_{cun})
f_{cre}	=	stress on returning strain (ε_{cre})
f_{cun}	=	stress on FRP confined concrete envelope at unloading strain (ε_{cun})
f_{cc}^{CRC}	=	compressive strength of confined concrete specimen
f_{cc}^{CPC}	=	compressive strength of confined plain concrete
f_{cc}^{URC}	=	compressive strength of unconfined reinforced concrete
H	=	height of the specimen
L_k	=	number of CFRP layers per each strip
S_j	=	number of strips along the specimen
SG	=	Strain gage
t_f	=	thickness of the wet lay-up CFRP sheet
UPC	=	unconfined plain concrete
URC	=	unconfined reinforced concrete
W_i	=	strip width
ε_{cc}	=	concrete axial compressive strain at f_{cc}
ε_{cc}^{CRC}		axial strain at compressive strength of confined reinforced concrete (f_{cc}^{CRC})
ε_{cc}^{CPC}		axial strain at compressive strength of confined plain concrete (f_{cc}^{CPC})
ε_{cc}^{URC}	=	axial strain at compressive strength of unconfined reinforced concrete (f_{cc}^{URC})
ε_{co}	=	axial strain at compressive strength of unconfined plain concrete (f_{co})
ε_{cpl}	=	concrete plastic strain
ε_{cre}	=	strain on the FRP confined concrete envelope corresponding to the return point
ε_{cun}	=	strain on FRP confined concrete envelope at unloading (reversal) point

ε_{fm} = Average tensile strain in the CFRP fiber's direction
ε_{fmax} = maximum tensile strain in the CFRP fiber's direction
ε_{su} = Steel ultimate strain
ρ_f = CFRP volumetric ratio
σ_{sy} = Steel yield stress
σ_{su} = Steel tensile strength

TABLES AND FIGURES

List of Tables:

Table 1 - Experimental program

Specimen designation (W*i*L*k*_c/m)	Loading type	W [mm]	s' [mm]	L	Confinement arrangement
W45L3_c	cyclic	45	55	3	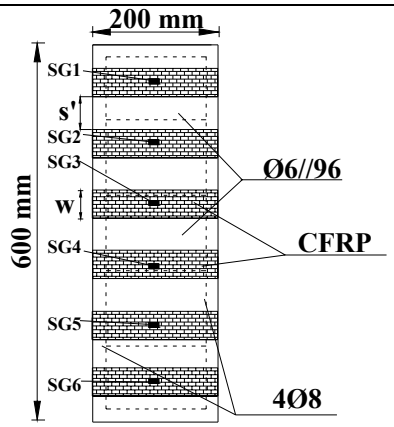
W45L3_m	monotonic				
W45L5_c	cyclic			5	
W45L5_m	monotonic				
W60L3_c	cyclic	60	40	3	
W60L3_m	monotonic				
W60L5_c	cyclic			5	
W60L5_m	monotonic				
W600L3_c	cyclic	600	-	3	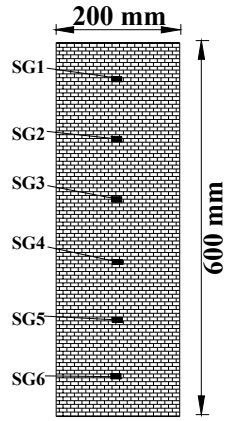
W600L3_m	monotonic				

Table 2 - Main indicators of the effectiveness of the confinement systems

Specimen designation	ρ_f[%]	f_{cc} (MPa)	$\frac{f_{cc}^{Conf}}{f_{cc}^{URC}}$	ε_{cc}	$\frac{\varepsilon_{cc}^{Conf}}{\varepsilon_{cc}^{URC}}$	ε_{fmax}					
						SG1	SG2	SG3	SG4	SG5	SG6
UPC_c	-	29.10	-	-0.003	-	-	-	-	-	-	-
UPC_m		30.36	-	-0.003	-	-	-	-	-	-	-
URC_c	-	27.50	-	-0.002	-	-	-	-	-	-	-
URC_m		27.38	-	-0.004	-	-	-	-	-	-	-
W45L3_c	0.31	44.40	1.61	-0.018	9.00	0.006	0.010	0.012	0.010	0.011	0.007
W45L3_m		40.97	1.50	-0.015	3.75	0.006	0.007	0.009	0.006	0.005	0.003
W45L5_c	0.51	50.74	1.85	-0.024	12.00	0.006	0.009	0.009	0.007	0.005	0.003
W45L5_m		54.14	1.98	-0.025	6.25	0.009	0.004	0.007	0.008	0.009	0.006
W60L3_c	0.41	48.84	1.78	-0.019	9.50	0.004	0.005	-	0.005	0.007	-
W60L3_m		51.83	1.89	-0.019	4.75	0.011	0.010	0.009	0.007	-	0.004
W60L5_c	0.68	55.64	2.02	-0.020	10.00	0.010	0.006	0.005	0.003	-	0.005
W60L5_m		66.27	2.42	-0.028	7.00	-	0.004	0.009	0.009	0.01	0.008
W600L3_c	0.68	73.70	2.68	-0.025	12.50	0.010	0.008	0.005	0.006	-	0.009
W600L3_m		58.01	2.12	-0.014	3.50	-	0.006	0.005	0.006	0.005	-

List of Figures:

a) b) c)

Figure 1- Confinement arrangements: a) strips of 45 mm width; b) strips of 60 mm width; c) full wrapping

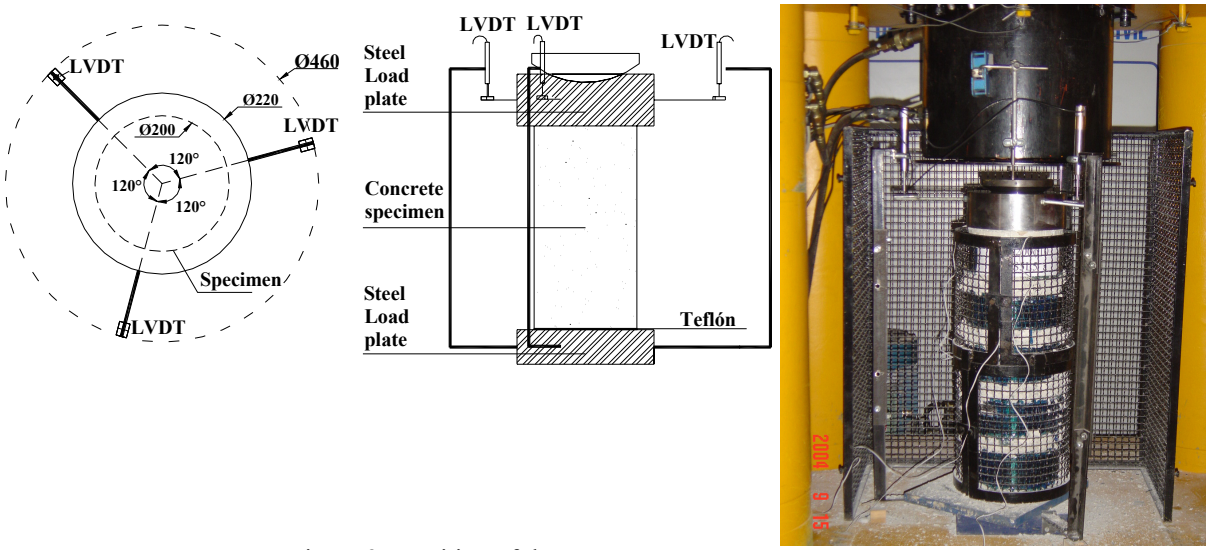

Figure 2 - Position of the LVDTs.

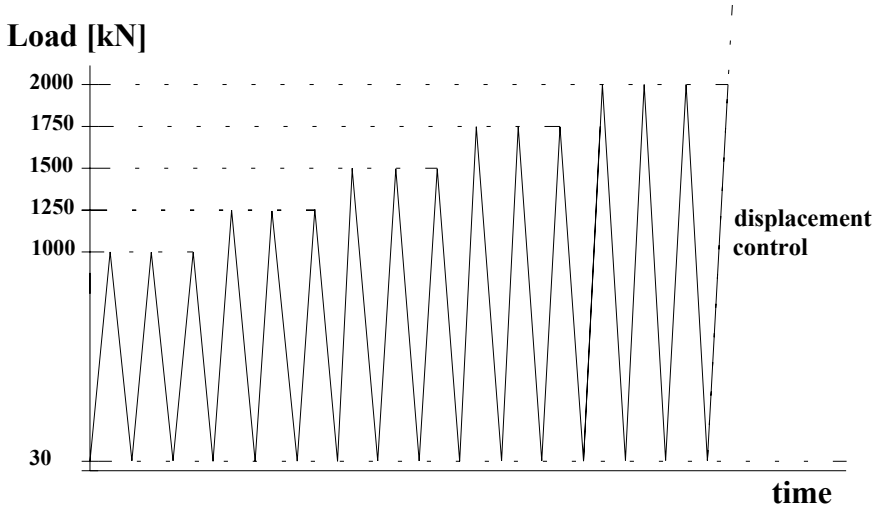

Figure 3 - Cyclic loading configuration

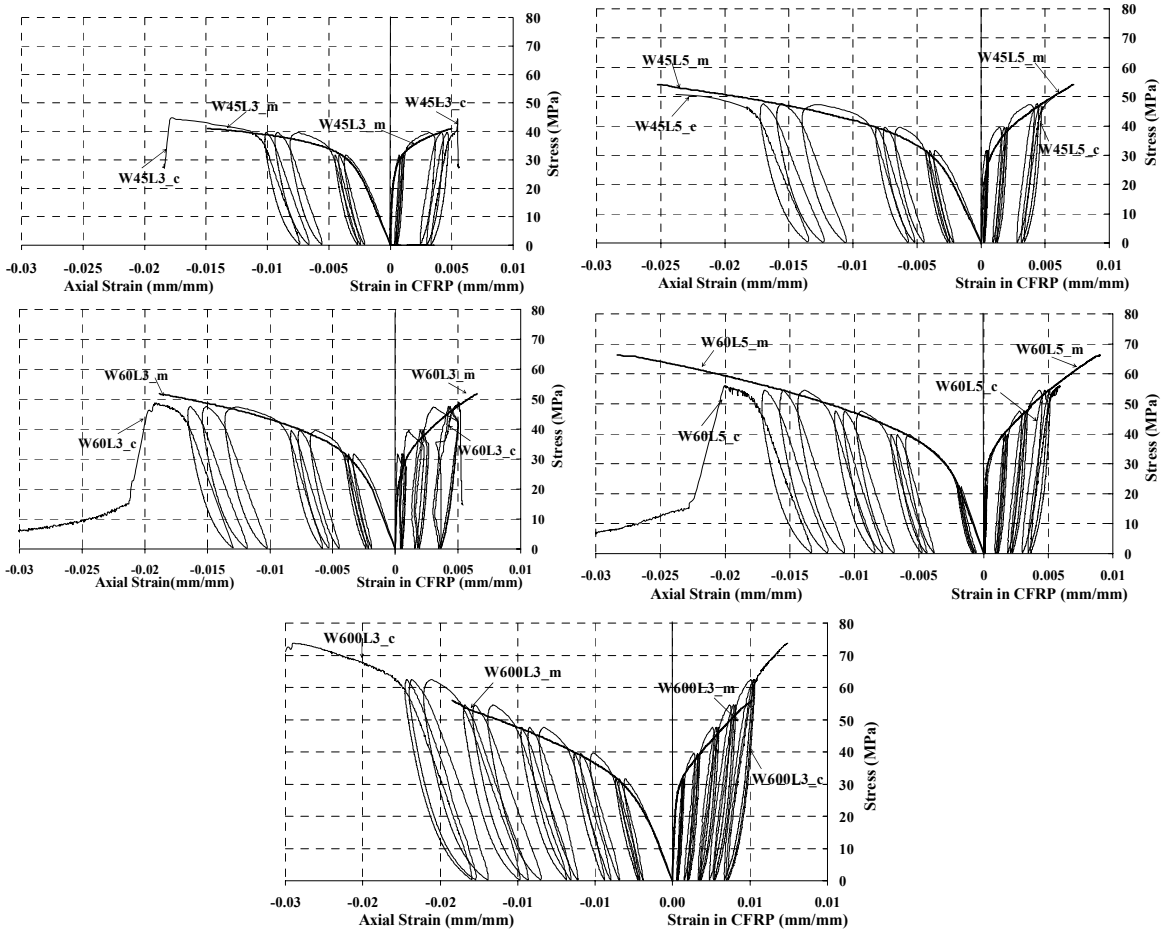

Figure 4: Relationship between concrete stress and both the axial strain and the CFRP strain for the monotonic and cyclic tests

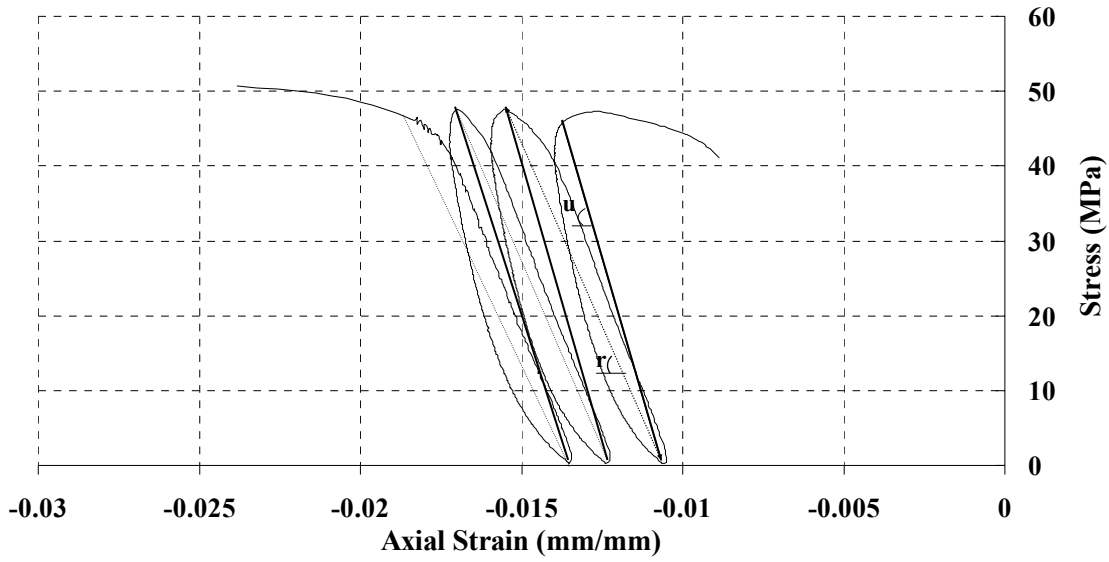

Figure 5: Procedure to evaluate the stiffness for unloading and reloading phases.

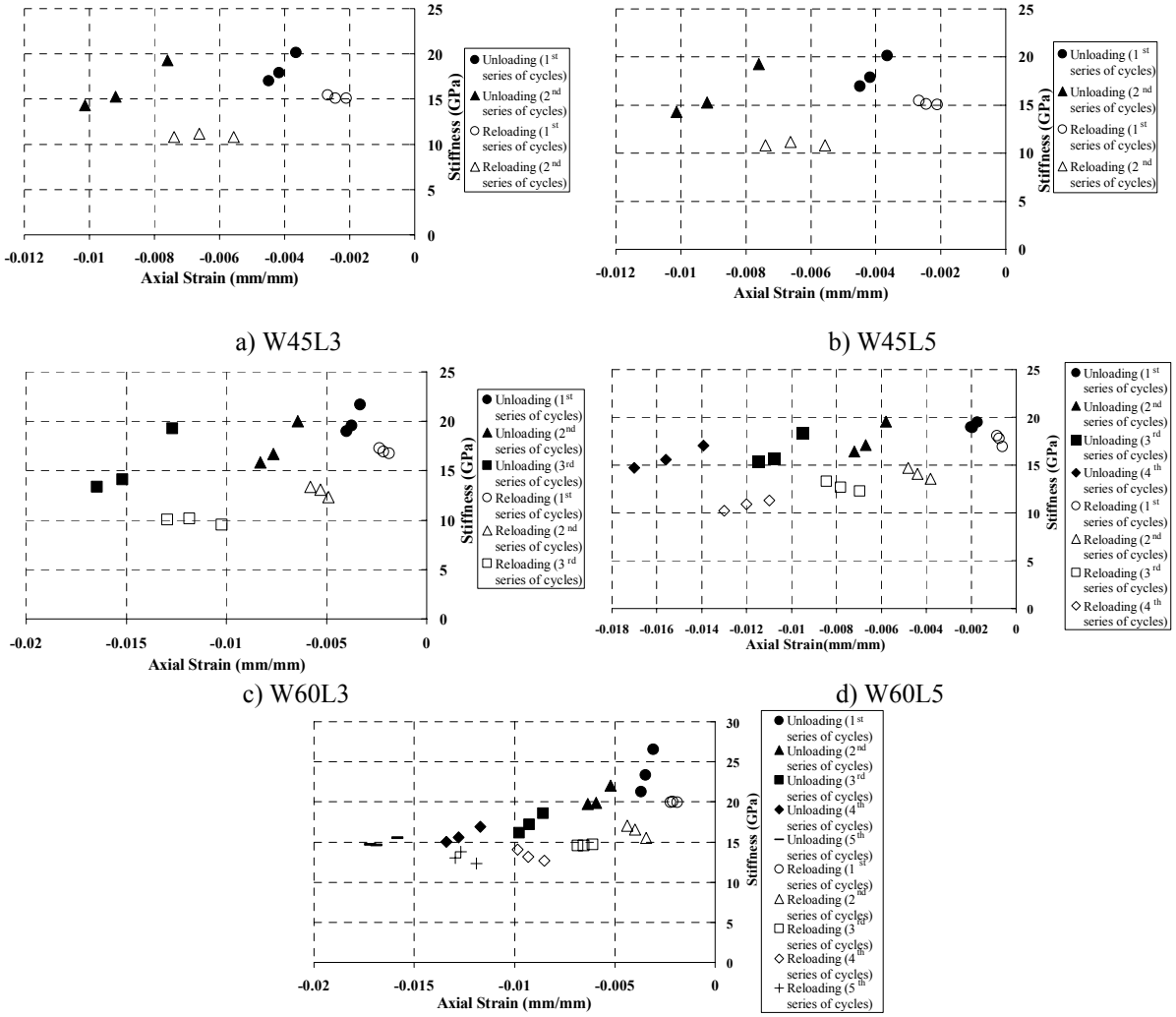

a) W45L3

b) W45L5

c) W60L3

d) W60L5

e) W600L3

Figure 6: Variation of the stiffness of the unloading and reloading branches in the cyclic tests

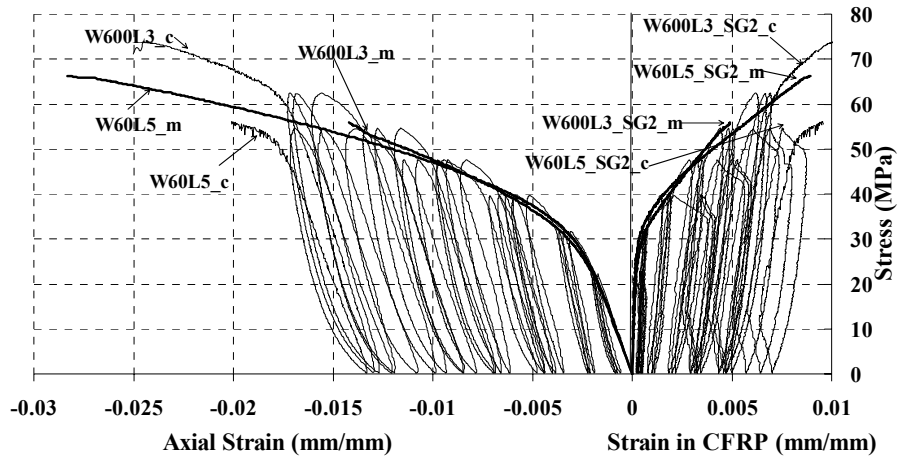

Figure 7: Relationship between the concrete stress and both the concrete axial strain and the CFRP strain in series with equal ρ_f: W60L5 and W600L3

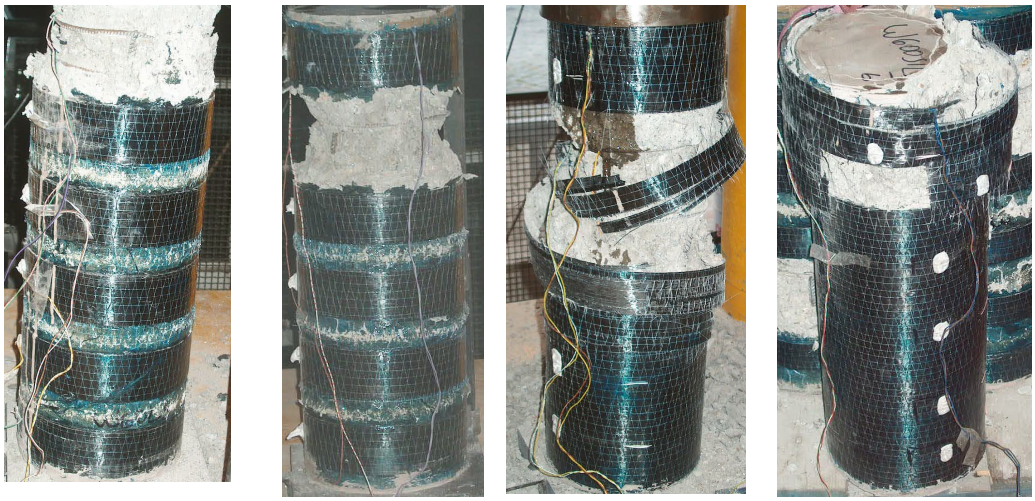

W60L5_c W60L5_m W600L3_c W600L3_m

Figure 8: Failure modes of specimens with equal ρ_f

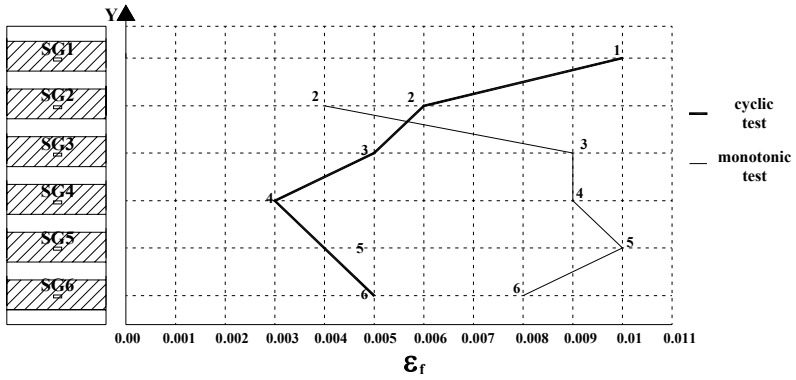

a) W60L5

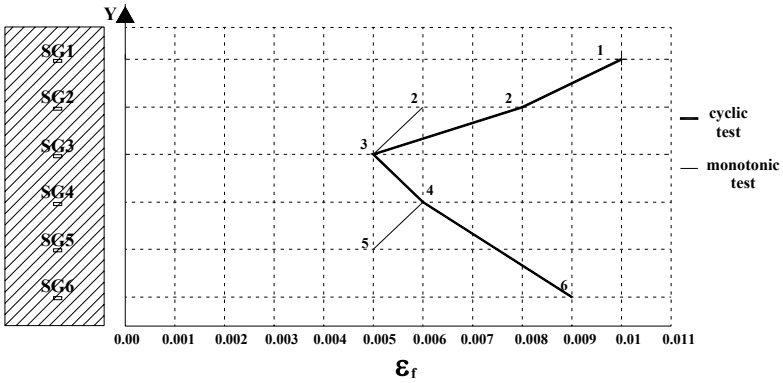

b) W600L3

Figure 9: Tensile strains in the CFRP for specimens: a) W60L5; b) W600L3.

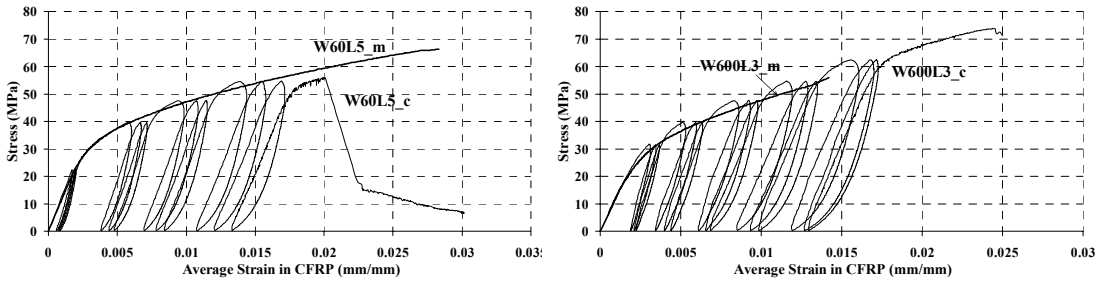

a) W60L5 b) W600L3

Figure 10: Relation between stress, σ_c, and axial average strain in CFRP, ε_c, under monotonic and cyclic tests, for the specimen: a) W60L5; b) W600L3.

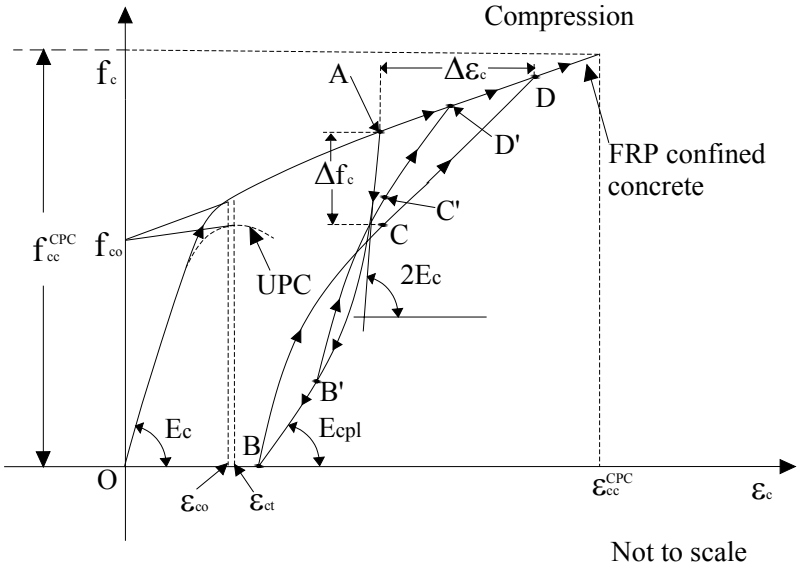

Figure 11: Schematic representation of the FRP-confined concrete constitutive model.

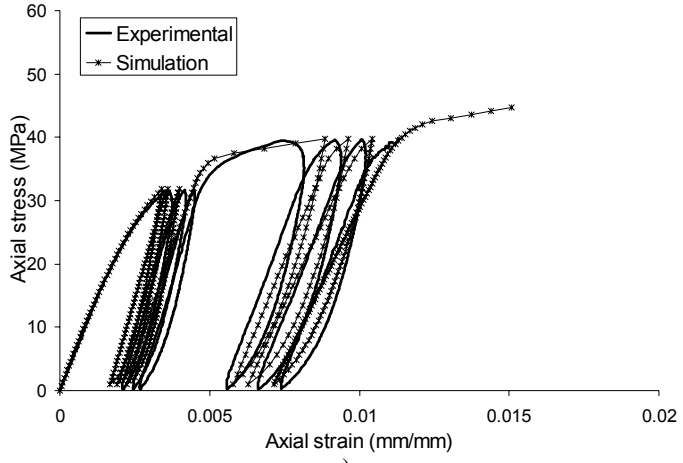

a)

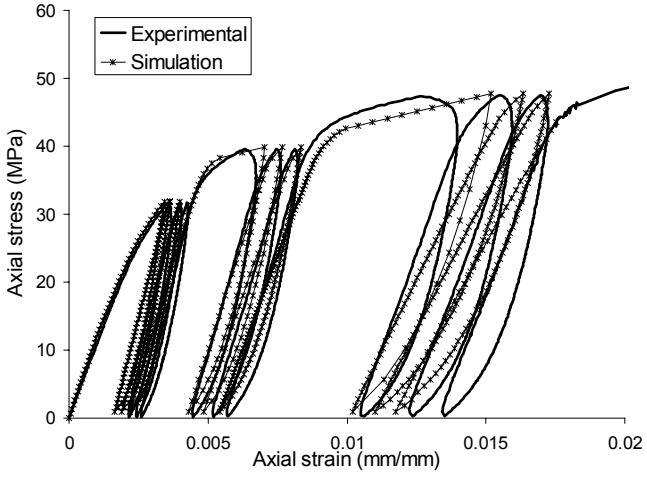

b)

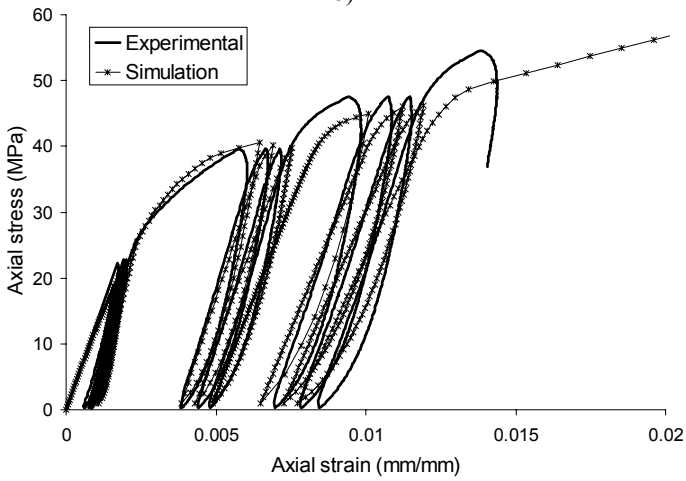

c)

Figure12: Numerical simulation of: a) W45L3_c, b) W45L5_c, and c) W60L5_c.